Egyptian Journal of Radiology and Nuclear Medicine

RESEARCH

Open Access

Diffusion tensor magnetic resonance imaging in differentiation of breast lesions

Esraa Saleh Amin[1*], Fatma Anas Elsharawy[1], Mohamed Ali Mlees[2], Haytham Haroun EL-Saeid[1] and Mohammed Fathy Dawoud[1]

Abstract

Background Diffusion tensor imaging (DTI) is a novel approach which uses extra gradients to quantify diffusion in several directions (at least six). The purpose of this research was to determine the role of diffusion tensor magnetic resonance imaging in breast lesion differentiation.

Results Apparent diffusion coefficient (ADC) values were significantly lower in malignant than benign lesions, with a cut-off value of 1.21×10^{-3} mm^2/s, this gives a sensitivity of 88.46%, specificity 87.50% and accuracy 86.7%. Values of fractional anisotropy (FA) were higher significantly in malignant compared to benign lesions with a 0.15 cut-off value, has a 95.83% sensitivity, 96.15% specificity, and 95.6%, accuracy. Values of RA were significantly higher in malignant (0.180 ± 0.068) compared to benign lesions, with 0.13 cut-off value. Sensitivity, specificity, and accuracy were, respectively, 91.69%, 92.31%, and 90.2%. Values of $\lambda 1$ were significantly lower in malignant ($1.4 \pm 0.453 \times 10^{-3}$ mm^2/s) than in benign ($2.19 \pm 0.659 \times 10^{-3}$ mm^2/s) lesions with a cut-off value of 1.71×10^{-3} mm^2/s. Sensitivity and specificity were, respectively, 95.83 and 96.15%. The combined evaluation by (dynamic contrast enhancement) Sensitivity improved to 100% with DCE and DTI readings, while specificity remained at 95.6%.

Conclusions DTI breast imaging is a noninvasive procedure which demonstrated a high potential utility for cancer detection and serving as a standalone technique or in conjunction with DCE-MRI, the discriminating values of FA, $\lambda 1$ and $\lambda 1$–$\lambda 3$ were high. Their measurements were strongly associated with identification breast malignancy and combined evaluation by DTI parameters and DCE-MRI DTI enhanced the sensitivity, lowered the rate of false-negatives, and completely improved the accuracy of breast lesions differential diagnosis.

Keywords Diffusion tensor magnetic resonance imaging, Breast lesions, Fractional anisotropy, Relative anisotropy

Background

Breast cancer is the most a frequent kind of cancer in females globally and is expected to be the second leading reason of death due to cancer [1, 2]. While the prevalence of breast cancer has grown across the previous two decades, the death rate has decreased significantly. Hence, early identification and precise differentiation of benign and malignant breast tumors perform a critical function in determining treatment selections and the efficacy of the chosen treatment technique [3].

Mammography and ultrasound are both well-established imaging techniques for diagnosing breast cancer [4]; however, in certain instances, these imaging techniques might produce equivocal results in which breast cancer cannot be ruled out [1]. Due to its exceptional sensitivity and contrast between soft and hard tissues, magnetic resonance imaging (MRI) can be utilized as a procedure for resolving problems to prevent or steer biopsies [5].

*Correspondence:
Esraa Saleh Amin
esraa.saleh@med.tanta.edu.eg
[1] Radiodiagnosis and Medical Imaging Department, Faculty of Medicine, Tanta University, El-Nahas St, Tanta 31512, Egypt
[2] Surgical Oncology Department, Faculty of Medicine, Tanta University, Tanta, Egypt

When dense breast tissue is seen on a mammogram, MRI of breast is a very sensitive imaging technique for cancer breast diagnosis. Additionally, it has been approved for use in various therapeutic conditions, for instance, screening females at risk and evaluation of breast cancer pre-to-surgical intervention [6].

Diffusion tensor imaging (DTI) is a new approach that makes use of extra gradients to quantify diffusion in several directions (at least six). This allows for the three-dimensional (3D) space quantification of diffusion and to determine the degree to which water diffuses in an anisotropic manner inside a tissue, quantified with the parameters relative anisotropy (RA) and fractional anisotropy (FA) [7].

In DTI sequence, mean diffusivity (MD) is described as an average of the apparent diffusion coefficient (ADC) values in three orthogonal directions, while another DTI indicator, FA, is a scalar number between 0 and 1 that quantifies the anisotropy degree in the process of diffusion. A value of zero indicates isotropic diffusion, which is unfettered (or equally limited) in every way. A value of one indicates that diffusion happens along a single axis and is completely prohibited in all other directions. Furthermore, DTI measures eigenvectors of diffusion in the three main x-, y-, and z-axes and their maximum, middle, and minimal eigenvalues ($\lambda 1$, $\lambda 2$, and $\lambda 3$), from which the MD, maximal anisotropy index ($\lambda 1$–$\lambda 3$), can be calculated [8].

This work aimed to identify the role of DTI MRI in breast lesions differentiation.

Methods

Setting of study

The MRI unit of the radio-diagnosis and imaging department at Tanta University Hospital during the period from October 2019 to October 2021.

This prospective observational cohort research was performed on 50 females aged 25–75 years old featured with breast complaints and/or abnormal sono-mammographic findings.

After a thorough discussion of the procedure's advantages and dangers, all patients involved in this research provided written informed permission. Any unexpected risks appeared during the study were timely disclosed to participants and the ethics committee.

The criteria for exclusion were as follows: previous breast surgery, chemotherapy or radiation and presence of cardiac pacemakers, ferromagnetic intracranial aneurysm clips.

Two groups of patients were formed: in accordance with histopathological diagnosis benign ($n=26$) and malignant ($n=24$).

Each patient had a thorough history taking, clinical examination, laboratory testing and breast MRI.

MRI

All MR imaging was carried out on a 1.5 Tesla (GE Health Care, Sigma HDX., W) using a bilateral breast coil. Each patient had the usual breast protocol, including:

Conventional MRI

- Axial T1-weighted imaging (TE 10 ms, TR 413 ms thickness of section 3 mm, 340_512 matrix, field of view [FOV] 457 mm).
- T2WI axial (TE 120 ms, TR 4,374 ms).
- T2WI axial with suppression of fat (TE 70 ms, TR 3,997 ms, 3-mm section thickness).
- STIR (TE = 30 ms, TR = 3000 ms, TI = 150 ms) in the transverse and sagittal plane; slice thickness: 4 mm; spacing: 1 mm; image matrix: 320 × 314. [9]

Diffusion weighted imaging (DWI)

In all patients, DWI was done using the following settings with b-values of 0, 800, and 1000 s/mm^2: TE 77 ms, TR 2,267 ms, section thickness of 5 mm, 256–256 matrix, 450 mm FOV, size of voxel 4.7–4.6 mm, sections number 30, gap section 0, anterior to posterior phase encoding) [1].

All patients had ADC maps produced, and the findings were compiled.

DTI

DTI was done in the axial plane using the procedure of medium three-dimensional (3D) DTI with the following parameters: 48 sections without a gap, TR 3802 ms, TE 106 ms, four excitations, 34 mm FOV, matrix 136_134, collection length 9 min 30 s, 3-mm section thickness, suppression of fat: recovery of spectral adiabatic inversion in 40 directions applied [9].

Dynamic contrast enhanced (DCE)

It was performed to 45 patients, a rapid spoiled gradient-recalled echo sequence in three dimensions with axial TWI was acquired (TE 1.22 ms, TR 4.19 ms 340_340 mm FOV, matrix of 448 340, thickness of section 0.9 mm, time of acquisition 6 min 42 s, Q-fat sat.) with gadolinium diethylenetriaminepentaacetic acid of a dosage of

Table 1 Age, clinical presentation, parity, family history, biopsy method, histopathologic diagnosis, and examination of the studied patients

		Patients ($n=50$)
Age (years)		
47.8 ± 14.6	25 to < 35	6 (12%)
	35 to < 45	9 (18%)
	45 to < 55	13 (26%)
	55 to < 65	12 (24%)
	65 to < 75	10 (20%)
Clinical presentation		
Breast mass	27 (54%)	
Mastalgia	12 (24%)	
Nipple discharge	7 (14%)	
Nipple retraction	4 (8%)	
Parity		
Nulliparous	22 (44%)	
Parous	28 (65%)	
Family history		
A positive family	23 (46%)	
Negative family	27 (54%)	
Biopsy method		
Tru-Cut	34 (68%)	
FNAC	6 (12%)	
Surgical excision	6 (12%)	
Tru-Cut and surgical excision	6 (12%)	
Histopathologic diagnosis		
Benign	26 (52%)	
Malignant	24 (48%)	
Diagnosis		
Benign		
Fibroadenoma	7 (16%)	
Fibroadenolipoma	1 (2%)	
Fibro-adenosis	6 (12%)	
Adenoma	4 (8%)	
Intra-ductal papilloma	3 (6%)	
Chronic granulomatous mastitis	2 (4%)	
Fat necrosis	3 (6%)	
Malignant		
Invasive ductal carcinoma	18 (36%)	
Invasive lobular carcinoma	2 (4%)	
Ductal carcinoma in situ	4 (8%)	

Data are presented as mean ± SD or frequency (%), FNAC: Fine needle aspiration cytology

0.1 mmol/kg administered across an indwelling catheter intravenously [1].

Clinical MRI interpretation

Lesion characteristics were assessed including size and enhancement pattern (focus, mass, non-mass enhancement [NME]) for masses, the form (round, irregular or oval), the edge (circumscribed, spiculated, or irregular), and the internal enhancement features (heterogeneous, homogeneous, presence of non-enhanced septa and rim enhancement), and non-masses were characterized in terms of their distribution and internal enhancement pattern.

Kinetic pattern of the worst curve type in DCE (characterized as the most suspect, with washout > plateau > persistence) was reported.

Final BI-RADS breast MRI lexicon evaluation.

DTI post-processing

All tensor-diffusion data were transferred and post-processed on the workstation.

Circular/free hand region of interest (ROI) was drawn manually along the lesion margin on the areas that show the greatest contrast enhancement and diffusion restriction, omitting regions that are hemorrhagic, cystic, or calcific.

- Each lesion's ADC was established by creating a ROI around it. If the lesion was larger than three centimeters in diameter, ADC values were obtained twice, and the average of the two values was utilized.
- The eigenvalues of diffusion tensor $\lambda 1$, $\lambda 2$, and $\lambda 3$ were then computed and evaluated using DTI parametric maps where $\lambda 1$, $\lambda 2$, and $\lambda 3$ are the eigenvalues of the diffusion tensor's maximum, intermediate, and minimum diffusion tensors, respectively,
- Additionally, the empirical parameter $\lambda 1$–$\lambda 3$ (maximum anisotropy index).
- MD was determined as the average of the three eigenvalues. MD represents the degree of mobility or hindrance of water molecules.
- FA and RA are diffusion anisotropy indices constructed from the eigenvalues of the diffusion tensor's terms**.** FA is a unitless index representing diffusion's degree of directionality, ranging from 0 (totally isotropic) to 1 (entirely directional) (completely anisotropic),
- Results were presented parametric maps of the eigenvalues in color-coded maps, and fiber tractography was drawn in the direction of mammary ducts.

Table 2 Relation of histopathological diagnosis to clinical data and correlation between MRI enhancement pattern and histopathological diagnosis correlation between type of kinetic curve and ADC values

		Benign (*n* = 26)	**Malignant (*n* = 24)**	***T* test *P*-value**
Clinical data	Age (years)	39.23 ± 10.70	57.25 ± 12.48	< 0.001*
	Parity Nulliparous (%)	35	65	< 0.001*
	Family history Positive (%)	38	62	< 0.001*
		(*n* = 23)	**(*n* = 22)**	**χ^2 Test *P*-value**
Enhancement pattern	Homogenous enhancing mass	13 (56.52%)	4 (18.18%)	< 0.01*
	Non mass enhancement	5 (21.74%)	9 (40.91%)	
	Heterogeneous enhancing mass	3 (13.04%)	9 (40.91%)	
	Focus enhancement	1 (4.35%)	0	
	Mass with ring enhancement	1 (4.35%)	0	
Total	23 (100%)	22 (100%)	100	
Kinetic curve	Type I	20 (86.95%)	1 (4.6%)	**< 0.001***
	Types 2 and 3	3 (13.05%)	21 (95.4%)	
Sens	Spec	PPV	NPV	Accuracy
95.4%	86.95%	95.4	86.95	91.1%
	Kinetic curve		**T-test**	
	Type I	**Type II and III**	***t***	***P*-value**
ADC ($\times 10^{-3}$ mm^2/s)	1.375 ± 0.124	1.068 ± 0.259	5.105	< 0.001*

Data are presented as mean ± SD or frequency (%), *: significant difference at *p* value < 0.05, ADC: apparent diffusion coefficient

Statistical analysis

SPSS v26 was used to conduct the statistical analysis (IBM Inc., Chicago, IL, USA). To compare the means and standard deviations of quantitative variables between the two groups, the unpaired Student's *t* test was utilized. Chi-square and Fisher's exact tests were used to analyze qualitative variables, which were provided as frequency and percentage (percentage). To be statistically significant, two-tailed *P* values less than 0.05 were required. This is an assessment of the test's sensitivity and specificity as well as the test's positive and negative predictive values (NPV). For this study, two-tailed *P* values of 0.05 or below were deemed statistically significant.

Results

Table 1 shows age, clinical presentation, parity, family history, biopsy method, histopathologic diagnosis, and examination of the studied patients

Malignant breast lesions were more common in patients with positive family history of breast cancer. Most of the mass with heterogeneous enhancing and non-mass enhancement patterns were in malignant (18 cases, 82%) that was statistically significant than benign lesions (eight cases, 35%) ($p < 0.01$). Correlation with histopathological results demonstrated that dynamic contrast enhancement MRI produced sensitivity, specificity and accuracy of 95.4%, 86.95% and 91.1%, respectively. Type I curve was significantly correlated with higher values of ADC, while type II and III show lower values of ADC (Table 2).

ADC values were significantly lower in malignant ($1.054 \pm 0.284 \times 10^{-3}$ mm^2/s) than in benign lesions ($1.388 \pm 0.228 \times 10^{-3}$ mm^2/s), with a cut-off value of 1.21×10^{-3} mm^2/s; this gives a sensitivity of 88.46%, specificity 87.50% and accuracy 86.7%. FA values were significantly higher in malignant (0.202 ± 0.065) than in benign lesions (0.129 ± 0.033) with a cut-off value of 0.15, gives sensitivity, specificity, and accuracy of 95.83%, 96.15%, and 95.6%, respectively. RA values were significantly higher in malignant (0.180 ± 0.068) than in benign lesions (0.117 ± 0.034), with a cut-off value of 0.13.

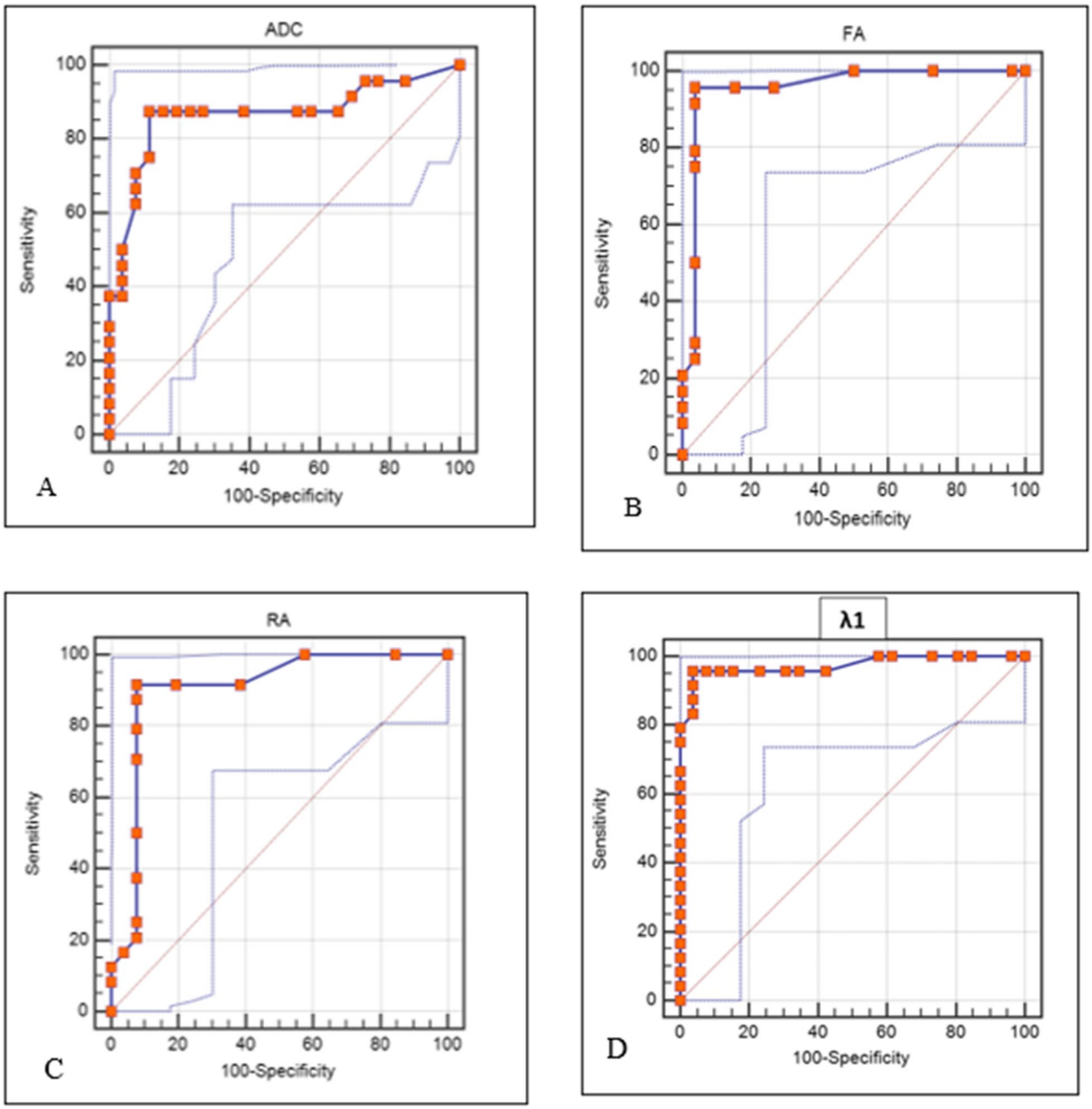

Fig. 1 **a** ROC curve for evaluation of ADC values, **b** FA values, **c** RA values and **d** $\lambda 1$ values in detection of malignant lesions. ADC: Apparent diffusion coefficient, FA: fractional anisotropy, RA: relative anisotropy, $\lambda 1$; maximum eigenvalue

Table 3 Correlation of eigenvalues in-between benign and malignant lesions and specificity and sensitivity of eigenvalues in detection of malignant lesions

DTI	Benign	Malignant	*T* test	
			t	*P*-value
λ1	2.192 ± 0.659	1.450 ± 0.453	11.808	< 0.001*
λ2	1.477 ± 0.377	1.157 ± 0.249	6.893	< 0.001*
λ3	1.461 ± 0.110	1.034 ± 0.174	10.449	< 0.001*
λ1–λ3	0.745 ± 0.102	0.545 ± 0.133	12.197	< 0.001*
	Cut-off	**Sensitivity %**	**Specificity %**	
λ1	≤ 1.7	95.83	96.15	
λ2	≤ 1.31	87.50	84.62	
λ3	≤ 1.19	90.67	89.00	
λ1–λ3	≤ 0.65	95.83	96.15	

Data are presented as mean ± SD, *: significant difference at *p* value < 0.05, DTI: diffusion tensor imaging. λ1, λ2, λ3: maximum, middle and minimum eigenvalues, respectively. λ1–λ3: maximum anisotropy index

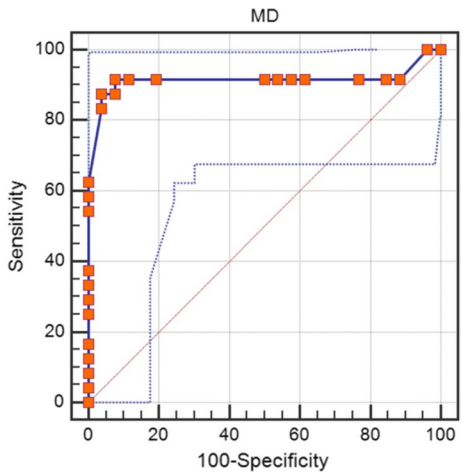

Fig. 2 ROC curve for evaluation of MD values in detection of malignant lesions

Sensitivity, specificity, and accuracy were 91.69%, 92.31%, and 90.2%, respectively. Values of $\lambda 1$ were significantly lower in malignant ($1.4 \pm 0.453 \times 10^{-3}$ mm^2/s) than in benign ($2.19 \pm 0.659 \times 10^{-3}$ mm^2/s) lesions with a cut-off value of 1.71×10^{-3} mm^2/s. Sensitivity and specificity were 95.83% and 96.15%, respectively (Fig. 1).

Values of $\lambda 1$–$\lambda 3$ were significantly lower in malignant ($0.545 \pm 0.133 \times 10^{-3}$ mm^2/s) than in benign ($0.745 \pm 0.102 \times 10^{-3}$ mm^2/s) lesions, with a cut-off value of 0.65×10^{-3} mm^2/s. Sensitivity and specificity were 95.83% and 96.15%, respectively (Table 3).

MD values were significantly lower in malignant ($1.232 \pm 0.442 \times 10^{-3}$ mm^2/s) than in benign lesions ($1.671 \pm 0.459 \times 10^{-3}$ mm^2/s), with a cut-off value of 1.41×10^{-3} mm^2/s. Sensitivity, specificity, and accuracy were 91.6%, 92.3%, and 91.4%, respectively Fig. 2.

Collectively, analyzing data of the present study, among DTI parameters, $\lambda 1$, $\lambda 1$–$\lambda 3$, and FA showed the highest diagnostic accuracy with sensitivity (95.83%) and specificity (96.15%). Following, DCE sensitivity and specificity were 86.95% and 95.4%, respectively, and MD with specificity and sensitivity of 91.67% and 92.31%, respectively (Table 4).

The sensitivity of DCE-MRI measurement and DTI measurements in 45 patients (who evaluated by DCE-MRI) is the same, each was 95.4%, while the specificity of DTI was higher (95.6%) than that of DCE-MRI (86.9%) (Table 5).

The combined evaluation by DCE and DTI values increased the sensitivity to 100%, but specificity still 95.6% (Table 6) (Figs. 3, 4, and 5).

Discussion

DTI is an innovative approach that makes use of extra gradients to quantify diffusion in many directions (at least six).This permits the characterization of diffusion in a space that is three-dimensional (3D) and the

Table 4 Diagnostic performance of DTI parameters

	Cut-off	Sensitivity %	Specificity %	PPV	NPV	Accuracy %
ADC	≤ 1.21	87.50	88.46	87.5	88.5	86.7
FA	> 0.15	95.83	96.15	95.8	96.2	95.6
RA	> 0.13	91.67	92.31	91.7	92.3	90.2
MD	≤ 1.41	91.67	92.31	91.7	92.3	91.4%
λ1	≤ 1.7	95.83	96.15	95.8	96.2	97.4
λ2	≤ 1.31	87.50	84.62	84.0	88.0	91.8
λ3	≤ 1.19	90.67	89.00	90.67	89.00	97.7
λ1–λ3	≤ 0.65	95.83	96.15	95.8	96.2	97.4

ADC: Apparent diffusion co-efficient. FA, RA: fractional and relative anisotropy, MD: mean diffusivity, λ1–λ3: maximum anisotropy index, λ1, λ2, λ3: maximum, middle and minimum eigenvalues, respectively

Table 5 Evaluation of diagnostic performance of DCE-MRI and DTI in comparison with histopathology ($n = 45$)

Diagnosis by DCE-MRI		Diagnosis by histopathology			
		Malignant lesion ($n = 22$)	Benign lesion ($n = 23$)		Total
Malignant lesion		21	3		24
Benign lesion		1	20		21
True positive	False positive	True negative	False negative	Sensitivity %	Specificity %
21	3	20	1	95.4	86.9
Diagnosis by DTI					
21	1	22	1	95.4	95.6

DCE-MRI: Dynamic contrast enhancement-magnetic resonance imaging, DTI: diffusion tensor imaging

Table 6 Evaluation of diagnostic performance of combined DCE-MRI images and DTI parameters in comparison with histopathology ($n = 45$)

Diagnosis by combined DCE and DTI		Diagnosis by histopathology			
		Malignant lesion ($n = 22$)	Benign lesion ($n = 23$)		Total
Malignant lesion		22	1		23
Benign lesion		0	22		22
Total		22	23		45
True positive	False positive	True negative	False negative	Sensitivity %	Specificity %
22	1	22	0	100	95.6

DCE: Dynamic contrast enhancement. DTI: diffusion tensor imaging

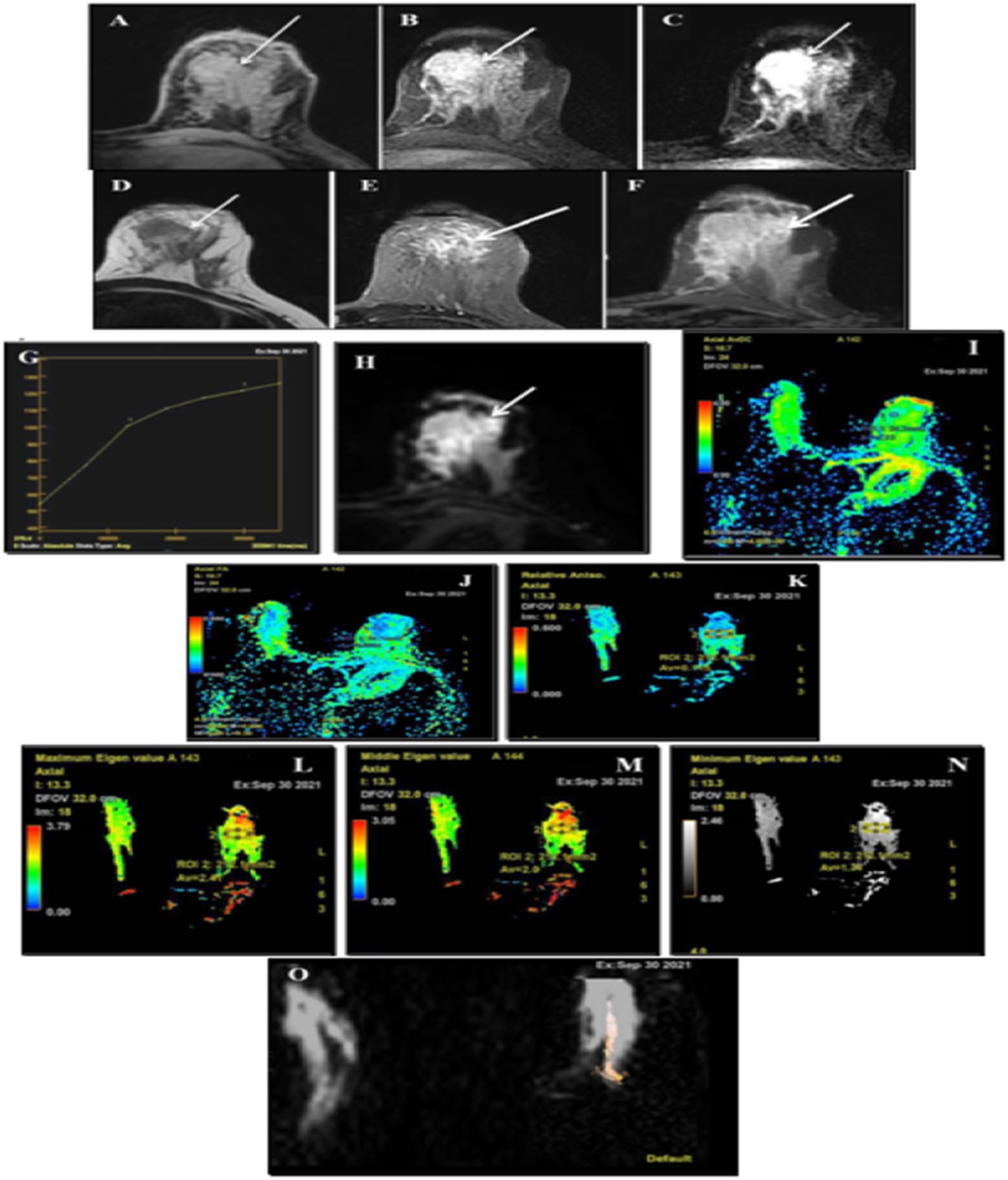

Fig. 3 **a** Axial T1WI FAT SAT pre-contrast: The mass displays isointense signal, **b** Axial T1WI post-contrast, **c** Post-subtraction images: Homogenous non-mass enhancement, **d** Axial T2WI: Low signal intensity, **e** Axial T2WI FS: The mass displays high signal intensity (no suppression), **f** Axial STIR: The mass displays high signal intensity, **g** kinetic curve: Type I, rising curve, **h** Axial DWI: The mass displays high signal, **i** ADC value = 1.37×10^{-3} mm^2/s (cut-off value of $< 1.21 \times 10^{-3}$ mm^2/s), **j** FA = 0.09 (cut-off value of > 0.15), **k** RA = 0.11 (cut-off value of > 0.13), **l** Maximum eigenvalue ($\lambda 1$) = 2.4×10^{-3} mm^2/s (cut-off value of $< 1.71 \times 10^{-3}$ mm^2/s), **m**: Middle eigenvalue ($\lambda 2$) = 2×10^{-3} mm^2/s (cut- off value of $< 1.31 \times 10^{-3}$ mm^2/s), **n** Minimum eigenvalue ($\lambda 3$) = 1.34×10^{-3} mm^2/s (cut- off value of $< 1.19 \times 10^{-3}$ mm^2/s) and **o** Fiber Tractography: Intact fibers suggesting benign nature of the mass. Provisional diagnosis by DCE-MRI and DTI parameters: Benign lesion. Histopathological diagnosis: Chronic granulomatous mastitis

quantification water diffusion in tissues that is anisotropic, quantified with the parameters FA and RA [10].

Diffusion tensor imaging (DTI) parameters $\lambda 1$, $\lambda 2$, $\lambda 3$, $\lambda 1$–$\lambda 3$, and MD in malignant tumors, in the present study, were significantly lower compared to benign lesions. This coincides with that reported in the work of Partridge et al. [7], Cakir et al. [11], Jiang et al. [12] and Onaygil et al. [13].

Jiang et al. [12] stated that MD and FA were shown to be substantially correlated with tissue cellularity in breast lesion, and the breast cancer had a higher cellularity than benign lesions.

Beppu et al. [14] suggested that the decrease in diffusion coefficients might be a result of malignant tissues' increased cellularity, which would limit the diffusion activity of water molecules in the extracellular compartment. Additionally, cancer cells obstructing ducts and lobules may lead to a drop in diffusion coefficients in all directions.

The assessment of eigenvalues ($\boldsymbol{\lambda}1$, $\boldsymbol{\lambda}2$, $\boldsymbol{\lambda}3$) may permit the three-dimensional description of diffusion, estimating the anisotropic water diffusion coefficient in a tissue [9].

Concerning the results of $\lambda 1$ measurements, the current work showed lower values in malignant tumors ($1.4 \pm 0.453 \times 10^{-3}$ mm^2/s) than benign lesions ($2.192 \pm 0.659 \times 10^{-3}$ mm^2/s) with a cut-off value of 1.71×10^{-3} mm^2/s, 95.83% sensitivity, and 96.15% specificity.

This is relatively comparable to the results of Onaygil et al. [13] who demonstrated that the mean value for benign and malignant lesions was $1.916 \pm 0.30 \times 10^{-3}$ mm^2/s and $1.276 \pm 0.19 \times 10^{-3}$ mm^2/s, respectively, with a value of cut-off point 1.59, sensitivity (97.8%), and specificity (87.2%). Additionally, 1 is capable of differentiating infiltrating breast cancer from ductal carcinoma in situ. Wang et al. [15] showed that invasive carcinomas exhibited a larger cellular density and a denser extracellular matrix than ductal carcinomas in situ, which hindered water transport.

Additionally, interstitial fibrosis was seen in the stroma of infiltrating breast cancer as a result of a desmoplastic response. This resulted in a decline of $\lambda 1$ in infiltrating breast cancer [15].

That is quite similar to the findings in the present study, where $\lambda 1$ value was obviously lower in invasive (1.2653×10^{-3} mm^2/s) than noninvasive lesions (1.623×10^{-3} mm^2/s).

Regarding $\lambda 2$ and $\lambda 3$ values, our study showed significantly higher value in benign (1.477 ± 0.377 and $1.461 \pm 0.410 \times 10^{-3}$ mm^2/s, respectively) than in malignant (1.157 ± 0.249 and $1.034 \pm 0.274 \times 10^{-3}$ mm^2/s) lesions, respectively, with cut-off values of 1.31 and 1.19×10^{-3} mm^2/s, respectively. Sensitivity and specificity of $\lambda 2$ were 87.50% and 84.62% and those for $\lambda 3$ were 90.6% and 89%, respectively.

There is a great similarity with the finding of Onaygil et al. [13] who concluded that the mean value of $\lambda 2$ and $\lambda 3$ in benign lesions was 1.686 ± 0.28 and $1.466 \pm 0.27 \times 10^{-3}$ mm^2/s, respectively, while in malignant lesions, the mean value of $\lambda 2$ and $\lambda 3$ were 1.016 ± 0.20 and $0.816 \pm 0.24 \times 10^{-3}$ mm^2/s, respectively. The cut-off value of $\lambda 2$ was 1.20×10^{-3} mm^2/s with a specificity of 95.7% and a sensitivity of 95.6%. The cut-off value of $\lambda 3$ was 1.06×10^{-3} mm^2/s giving specificity 93.6% and sensitivity 95.6%.

The diagnostic performance of maximum anisotropic index ($\lambda 1$–$\lambda 3$) in distinguishing malignant and benign lesions was evaluated, and we obtained lower values in malignant breast lesions ($0.545 \pm 0.133 \times 10^{-3}$ mm^2/s) compared to benign lesions ($0.745 \pm 0.102 \times 10^{-3}$ mm^2/s) with a cut-off value of 0.65×10^{-3} mm^2/s. The maps of $\lambda 1$–$\lambda 3$ provided a high sensitivity (95.83%) and specificity (96.15%).

These results agree with that previously reported by others (Eyal et al. [16] and Onaygil et al. [13]). However, Luo et al. [17] reported that maximum anisotropic index ($\lambda 1$–$\lambda 3$) did not demonstrate a significant difference between malignant and benign lesions.

In the present work, the mean MD values were significantly lower in malignant ($1.232 \pm 0.442 \times 10^{-3}$ mm^2/s) than in benign ($1.671 \pm 0.459 \times 10^{-3}$ mm^2/s) breast lesions with a cut-off value of 1.41×10^{-3} mm^2/s giving a sensitivity of 91.6% and a specificity of 92.3%.

(See figure on next page.)

Fig. 4 **a** Axial T1WI FS pre-contrast: Lesion displays intermediate signal intensity, **b** Axial T1WI post-contrast, **c** Post-subtraction images: Homogenous enhancement lesion. **d** Axial T2WI: The lesion displays low signal intensity, **e** Axial STIR: The lesion displays high signal Intensity, **f** kinetic curve: Type III, washout curve, **g** DWI: The lesion displays high signal intensity, **h** ADC value = 1.09×10^{-3} mm^2/s (cut-off value of < 1.21×10^{-3} mm^2/s,. **i** FA = 0.22 (cut-off value of > 0.15), **j** RA = 0.25 (cut-off value of > 0.13), **k** Maximum eigenvalue ($\lambda 1$) = 1.31×10^{-3} mm^2/s (cut-off value of < 1.71×10^{-3} mm^2/s), **l** Middle eigenvalue ($\lambda 2$) = 1.16×10^{-3} mm^2/s (cut-off value of < 1.31×10^{-3} mm^2/s), **m** Minimum eigenvalue ($\lambda 3$) = 1.06×10^{-3} mm^2/s (cut-off value of < 1.19×10^{-3} mm^2/s) and **n** Fiber Tractography: Distortion and discontinuity of fiber tracts, suggesting malignant lesion. Provisional diagnosis by DCE-MRI and DTI parameters: Malignant lesion. Histopathological diagnosis: Invasive ductal carcinoma

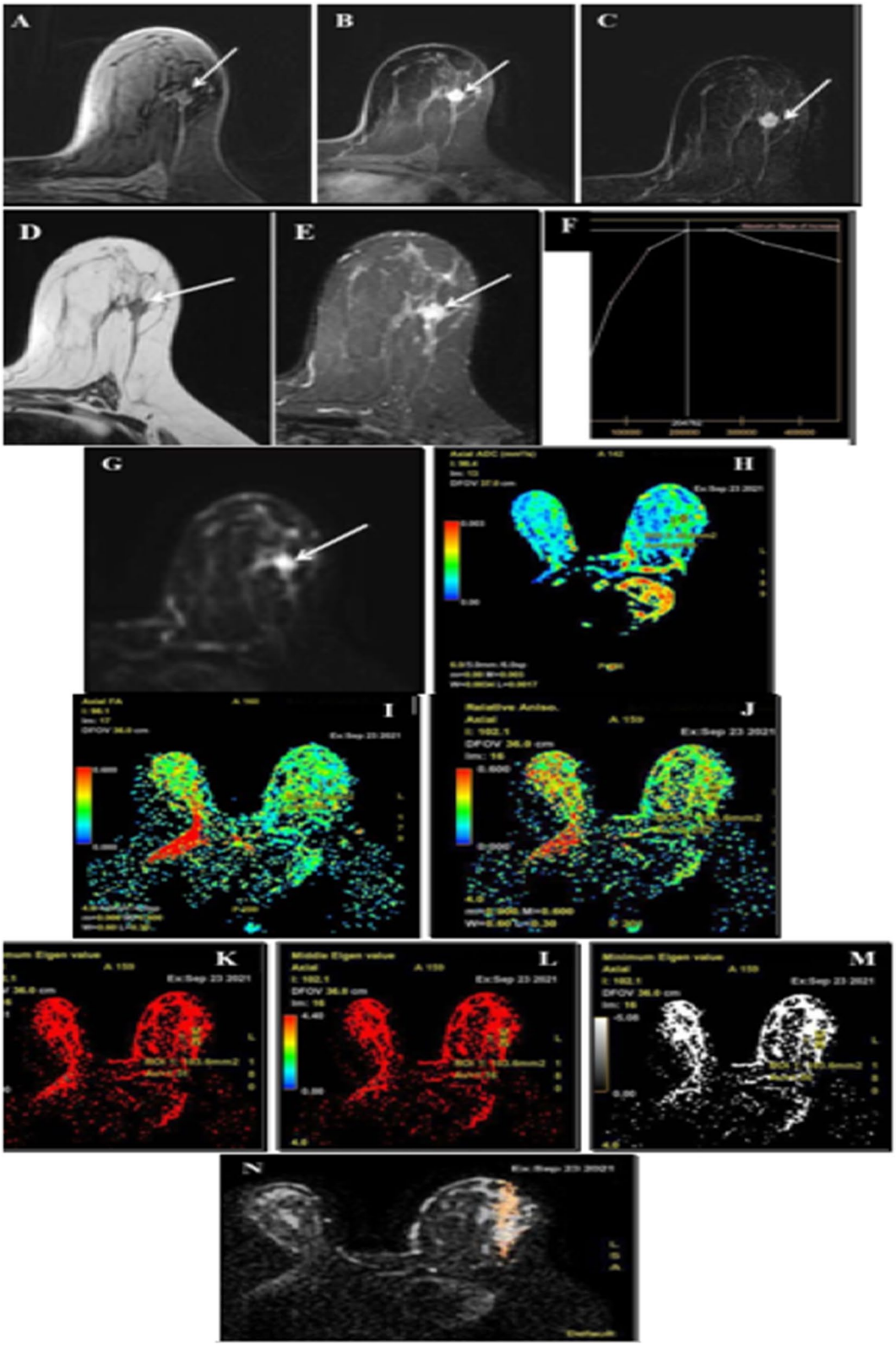

Fig. 4 (See legend on previous page.)

In agreement, Onaygil et al. [13] showed that the mean value of MD in benign lesions was 1.686 ± 0.27 and in malignant lesions was $1.036 \pm 0.19 \times 10^{-3}$ mm^2/s, with a cut-off value of 1.24×10^{-3} mm^2/s giving a sensitivity of 95.6% and a specificity of 93.6%.

Analyzing the results of the present study and evaluating ADC and DTI parameters as discriminators of benign and malignant lesions, ADC sensitivity and specificity were 88.4% and 87.5%, respectively. DTI parameters $\lambda 1$, $\lambda 1$–$\lambda 3$, and FA obviously shows higher sensitivity (95.83%) and specificity (96.15%).

However, this is different form that reported by Tsougos et al. [3] who evaluated parameters of the ADC and DTI as discriminators between benign and malignant tissues. The ADC has a sensitivity of 85% and a specificity of 84.4%, respectively, while those of FA were 65.8% and 67.4%, respectively.

Among the variable studied parameters and reviewing ROC curve analysis, we concluded that the $\lambda 1$, $\lambda 1$–$\lambda 3$ and FA demonstrated the highest diagnostic efficiency (sensitivity, 95.83% and specificity, 96.15%), followed by DCE (sensitivity, 95.4% and specificity, 86.95%) then MD values (sensitivity, 92.31% and specificity, 91.67%).

Concerning the research that examined the role of DTI in differentiating breast lesions, Tsougos et al. [3] reported that MD and $\lambda 1$ are the most discriminative DTI parameters for breast lesion detection (sensitivity of 82.5% and specificity of 81.4%).

Wang et al. [15] showed that ADC and $\lambda 1$ have the greatest discriminative values, followed by $\lambda 1$– $\lambda 3$, with $\lambda 1$ and $\lambda 2$ performing extremely similarly to ADC in terms of sensitivity and specificity.

The discrepancy between our results and those of the previous studies may be partly attributed to the heterogeneity related to *b*-values.

Different selected *b*-values, and the number of gradient directions varies between studies, which may have an effect on the estimation of parameters of DTI [18]. In our study, we used *b*-values of 0, 800 and 1000 s/mm^2 and 40 directions.

In comparison with previous studies, Luo et al. [17] used *b*-value of 0, 100, 800, and six directions, Onaygil et al. [13] used *b*-value of 0, 700, and 30 directions, while Cakir et al. [11] used *b*-value of 0, 1000, and 16 directions.

On comparing the diagnostic performance of DTI and DCE in 45 patients who are examined by both techniques, DTI achieved a higher specificity than DCE-MRI, and it showed about 95.6% compared to 86.9% of DCE; both showed the same sensitivity 95.4%. The combined evaluation increased the sensitivity to 100% and specificity of DCE to 95.6%.

This agrees with results of a study done by Onaygil et al. [13] who showed that addition of DTI parameters to DCE-MRI increases the specificity of DCE-MRI from 83.0 to 93.6% and sensitivity to 100%.

Wang et al. [15] also revealed that adding DTI to DCE-MRI might improve performance of diagnosis, as the specificity of DCE-MRI increased from 84 to 94% when DTI was included. Therefore, using DTI in conjunction with traditional breast cancer in routine clinical practice, DCE-MRI may help minimize the frequency of needless benign biopsies [15].

Limitations: The sample size was relatively small. The study was in a single center.

Conclusions

Values of FA and RA were significantly higher in malignant than benign lesions, values of ADC, $\lambda 1$, $\lambda 2$, $\lambda 3$, $\lambda 1$–$\lambda 3$, and MD were significantly lower in malignant than benign breast lesions, breast DTI is a noninvasive method that demonstrated a high potential utility for cancer detection and serving as a standalone technique or in conjunction with DCE-MRI, the discriminating values of FA, $\lambda 1$ and $\lambda 1$–$\lambda 3$ were high. Their measurements were strongly associated with identification breast malignancy and combined evaluation by DTI parameters and DCE-MRI DTI enhanced the sensitivity, lowered the rate of false-negatives, and completely improved the accuracy of breast lesions differential diagnosis.

(See figure on next page.)

Fig. 5 **a** Axial T1WI post-contrast, **b** Post-subtraction imaging: An oval-shaped lesion with homogenous enhancement, **c** Axial T2WI: The lesion displays low signal intensity, **d** Axial T2WI FS: The lesion displays high signal, no fat suppression, **e** Axial STIR: The lesion displays high signal intensity, **f** kinetic curve: Type I, rising curve, **g** Axial DWI: The lesion displays high signal intensity, **h** ADC value = 1.5×10^{-3} mm^2/s (cut-off value of < 1.21×10^{-3} mm^2/s), **i** FA = 0.05 (cut-off value of > 0.15), **j** RA = 0.10 (cut-off value of > 0.13), **k** Maximum eigenvalue ($\lambda 1$) = 2.21×10^{-3} mm^2/s (cut-off value of < 1.71×10^{-3} mm^2/s), **l** Middle eigenvalue ($\lambda 2$) = 1.39×10^{-3} mm^2/s (cut-off value of < 1.31×10^{-3} mm^2/s), **m** Minimum eigenvalue ($\lambda 3$) = 1.2×10^{-3} mm^2/s (cut-off value of < 1.19×10^{-3} mm^2/s) and **n** Fiber Tractography: Almost intact fiber tracts, suggesting benign lesion. Provisional diagnosis by DCE-MRI and DTI parameters: Benign lesion. Histopathological diagnosis: Fibroadenoma

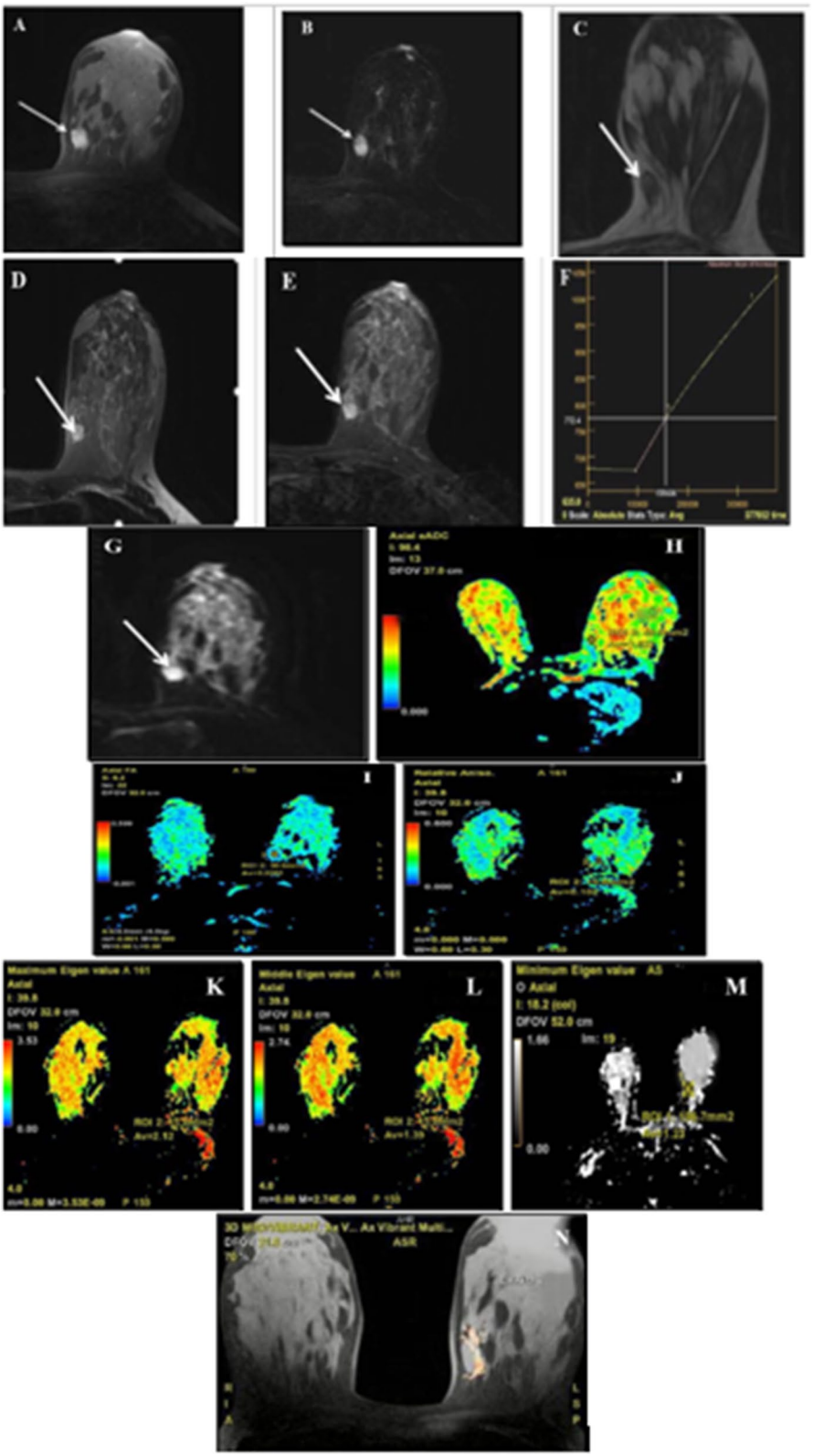

Fig. 5 (See legend on previous page.)

Abbreviations

DTI	Diffusion tensor imaging
ADC	Apparent diffusion coefficient
FA	Fractional anisotropy
RA	Relative anisotropy
DCE	Dynamic contrast enhanced
MRI	Magnetic resonance imaging
MD	Mean diffusivity
DWI	Diffusion weighted imaging
NME	Non-mass enhancement
ROI	Region of interest

Acknowledgements
Not applicable.

Author contributions
MFD and HHE conceived and supervised the study; ESA and FAE were responsible for data collection. MAM and MFD analyzed and interpreted the data. All authors provided comments on the manuscript at various stages of development. All authors read and approved the final manuscript.

Funding
No funding was obtained for this study.

Availability of data and materials
Data and material are available on a reasonable request from the author.

Declarations

Ethics approval and consent to participate
It was approved by the ethics committee of Faculty of medicine, Tanta University, and it was started at October 2019 to October 2021. An informed written consent was obtained from the participants. Approval No. 32846/01/19.

Consent for publication
All authors give their consent for publication in the journal.

Competing interests
The authors declare no competing interests.

Received: 17 May 2022 Accepted: 23 August 2022
Published online: 31 January 2023

References

1. Abdelhady D, Abdelbary A, Afifi AH, Abdelhamid A-E, Hassan HHM (2021) Diffusion tensor imaging on 3-T MRI breast: diagnostic performance in comparison to diffusion-weighted imaging. EJRNM 52(1):98–103. https://doi.org/10.1186/s43055-021-00473-6
2. DeSantis CE, Ma J, Goding Sauer A, Newman LA, Jemal A (2017) Breast cancer statistics, 2017, racial disparity in mortality by state. CA Cancer J Clin 67(6):439–448. https://doi.org/10.3322/caac.21412
3. Tsougos I, Bakosis M, Tsivaka D, Athanassiou E, Fezoulidis I, Arvanitis D et al (2019) Diagnostic performance of quantitative diffusion tensor imaging for the differentiation of breast lesions at 3 T MRI. Clin Imaging 53:25–31. https://doi.org/10.1016/j.clinimag.2018.10.002
4. Kul S, Cansu A, Alhan E, Dinc H, Gunes G, Reis A (2011) Contribution of diffusion-weighted imaging to dynamic contrast-enhanced MRI in the characterization of breast tumors. AJR Am J Roentgenol 196(1):210–217. https://doi.org/10.2214/ajr.10.4258
5. Perry N, Broeders M, de Wolf C, Törnberg S, Holland R, von Karsa L (2008) European guidelines for quality assurance in breast cancer screening and diagnosis: fourth edition–summary document. Ann Oncol 19(4):614–22. https://doi.org/10.1093/annonc/mdm481
6. Wiederer J, Pazahr S, Leo C, Nanz D, Boss A (2014) Quantitative breast MRI: 2D histogram analysis of diffusion tensor parameters in normal tissue. MAGMA 27(2):185–193. https://doi.org/10.1007/s10334-013-0400-9
7. Partridge SC, Ziadloo A, Murthy R, White SW, Peacock S, Eby PR et al (2010) Diffusion tensor MRI: preliminary anisotropy measures and mapping of breast tumors. J Magn Reson Imaging 31(2):339–347. https://doi.org/10.1002/jmri.22045
8. Plaza MJ, Morris EA, Thakur SB (2016) Diffusion tensor imaging in the normal breast: influences of fibroglandular tissue composition and background parenchymal enhancement. Clin Imaging 40(3):506–511. https://doi.org/10.1016/j.clinimag.2015.12.001
9. El Ameen NF, Abdel Gawad EA, Abdel Ghany HS (2021) Diffusion-weighted imaging versus dynamic contrast-enhanced MRI: a new horizon for characterisation of suspicious breast lesions. Clin Radiol 76(1):80–85. https://doi.org/10.1016/j.crad.2020.08.031
10. Xu SH, Zhang J, Zhang Y, Zhang P, Cheng GQ (2021) Non-invasive cardiac output measurement by electrical cardiometry and M-mode echocardiography in the neonate: a prospective observational study of 136 neonatal infants. Transl Pediatr 10(7):1757–1764. https://doi.org/10.21037/tp-21-20
11. Cakir O, Arslan A, Inan N, Anık Y, Sarısoy T, Gumustas S et al (2013) Comparison of the diagnostic performances of diffusion parameters in diffusion weighted imaging and diffusion tensor imaging of breast lesions. Eur J Radiol 82(12):801–806. https://doi.org/10.1016/j.ejrad.2013.09.001
12. Jiang R, Zeng X, Sun S, Ma Z, Wang X (2016) Assessing detection, discrimination, and risk of breast cancer according to anisotropy parameters of diffusion tensor imaging. Med Sci Monit 22:1318–1328. https://doi.org/10.12659/msm.895755
13. Onaygil C, Kaya H, Ugurlu MU, Aribal E (2017) Diagnostic performance of diffusion tensor imaging parameters in breast cancer and correlation with the prognostic factors. J Magn Reson Imaging 45(3):660–672. https://doi.org/10.1002/jmri.25481
14. Beppu T, Inoue T, Shibata Y, Yamada N, Kurose A, Ogasawara K et al (2005) Fractional anisotropy value by diffusion tensor magnetic resonance imaging as a predictor of cell density and proliferation activity of glioblastomas. Surg Neurol 63(1):56–61. https://doi.org/10.1016/j.surneu.2004.02.034
15. Wang K, Li Z, Wu Z, Zheng Y, Zeng S, Linning E et al (2019) Diagnostic performance of diffusion tensor imaging for characterizing breast tumors: a comprehensive meta-analysis. Front Oncol 9:120–5. https://doi.org/10.3389/fonc.2019.01229
16. Eyal E, Shapiro-Feinberg M, Furman-Haran E, Grobgeld D, Golan T, Itzchak Y et al (2012) Parametric diffusion tensor imaging of the breast. Invest Radiol 47(5):284–291. https://doi.org/10.1097/RLI.0b013e3182438e5d
17. Luo J, Hippe DS, Rahbar H, Parsian S, Rendi MH, Partridge SC (2019) Diffusion tensor imaging for characterizing tumor microstructure and improving diagnostic performance on breast MRI: a prospective observational study. Breast Cancer Res 21(1):1–16
18. Lee JW, Kim JH, Kang HS, Lee JS, Choi JY, Yeom JS et al (2006) Optimization of acquisition parameters of diffusion-tensor magnetic resonance imaging in the spinal cord. Invest Radiol 41(7):553–559. https://doi.org/10.1097/01.rli.0000221325.03899.48

Publisher's Note